European Polymer Journal 124 (2020) 109470

Contents lists available at ScienceDirect

European Polymer Journal

journal homepage: www.elsevier.com/locate/europolj

Structural properties of vegetable oil thermosets: Effect of crosslinkers, modifiers and oxidative aging

Sebastián Anbinder[a], Cintia Meiorin[b], Carlos Macchi[a], Mirna A. Mosiewicki[b], Mirta I. Aranguren[b,*], Alberto Somoza[a,*]

[a] Instituto de Física de Materiales Tandil (UNCPBA) and CIFICEN (UNCPBA-CICPBA-CONICET), Pinto 399, B7000GHG Tandil, Argentina
[b] Instituto de Investigaciones en Ciencia y Tecnología de Materiales (INTEMA), Universidad Nacional de Mar del Plata (UNMdP) – CONICET, Av. Juan B. Justo 4302, (7600) Mar del Plata, Argentina

ARTICLE INFO

Keywords:
Vegetable oil thermosets
Bio-based resins
Structural properties
Aging conditions
Positron annihilation spectroscopy

ABSTRACT

The present work is focused on the study of the formulation effect of cationically polymerized vegetable oil thermoset on their aging behavior. Toward this aim, tung oil-based biopolymers were prepared using different comonomers or adding a modifier. Specifically, synthetic and natural comonomers (styrene, divinylbenzene and a methyl ester of tung oil) and a modifier (acrylated epoxidized soybean oil) were used to prepare different crosslinked samples with a fixed weight ratio of tung oil/comonomer (or modifier) = 70/30. The chemical aging suffered by the fatty acid segments of the matrix, which is known as autoxidation of unsaturated fatty acids in oils and alkyd resins, was followed by Fourier transformed infrared spectroscopy, dynamic-mechanical analysis, positron annihilation lifetime spectroscopy and thermogravimetric analysis. As a result, values of the glass transition temperature, the storage moduli, tanδ and the free nanohole volumes were obtained. To study the influence of the aging process on the network structures at molecular level, the evolutions of the experimental parameters mentioned were followed for one year at two different aging conditions: room temperature and 50 °C.

The chemical changes leading to nanostructural variations in all the studied samples are discussed in terms of the formed networks and the degradative processes during aging.

1. Introduction

The pressure of international policies and of the general public to reduce the consuming of petroleum derived polymers and the particular properties that can be obtained from bio-based monomers and precursors present new challenges in the R&D worldwide activities around the world. In the search of renewable sources for the synthesis of polymeric materials, vegetable oils have attracted, justifiably, the attention of different research groups. Triglycerides contain several functional groups that can be chemically used to generate materials of interest. They offer the basic raw material to the synthesis of a wide variety of precursors that can be utilized in different final applications. In particular, unsaturated vegetable oils can participate in reactions that involve the −C═C− bond. Tung oil is one of such unsaturated vegetable oils that has been traditionally used as a high performance drying oil. This triglyceride contains eleostearic acid as the main fatty acid component, having three conjugated unsaturations. Due to this particular characteristic, it can participate in cationic polymerizations to produce polymeric thermoset materials without need of any previous modification, as it is necessary in the case of other vegetable oils [1,2]. To tailor some properties to these systems, styrene and also mixtures with divinylbenzene were usually used as comonomers. However, these two reactives even being commodities are petroleum derived reagents and not ecofriendly, a reason why a search for biobased comonomers was considered. Methyl ester of tung oil obtained by methanolysis of tung oil was thus, a first choice since it could be easily obtained from the same base triglyceride. Acrylated epoxidized soybean oil (AESO) was also considered, since the acryl double bonds of this molecule easily react in radical polymerizations. However, it has been demonstrated that they are not reactive in cationic polymerizations; so in TO-based polymers AESO acts mainly as a modifier of the thermoset [2]. In such a way, the addition of these bio-molecules in the formulation allow to reduce the use of harmful monomers, increasing the bio-carbon content in the materials.

The use of unsaturated triglycerides in the preparation of thermoset structures lets open the possibility of some unsaturations remaining

* Corresponding authors.
E-mail addresses: marangur@fi.mdp.edu.ar (M.I. Aranguren), asomoza@exa.unicen.edu.ar (A. Somoza).

https://doi.org/10.1016/j.eurpolymj.2019.109470
Received 8 October 2019; Received in revised form 27 December 2019; Accepted 31 December 2019
Available online 02 January 2020

unreacted in the final material, which means that the material will be able to evolve in time due to the autoxidation process.

The oxidation of unsaturated oils can be described in a simplified way as a free radical mechanism, that leads in a first step, to the occurrence of hydroperoxides followed by the decomposition of these components that lead to the formation of low molecular weight oxidation products (such as aldehydes and ketones) and also to cross-linking through the fatty acid moieties [3–6]. The reaction mechanism involves two different reaction steps: a first one, very fast, which consists in a chain carrying carbon radical reacting with oxygen and a second one, slower, referring to the propagation step, where a peroxyl radical extracts hydrogen from an organic substrate [6]. The different rates depend on several factors such as temperature, light, presence of oxygen and moisture. The type of oil also influences the rate of oxidation.

Polymers from triglyceride oils are prepared *via* different polymerization methods, such as condensation, radical and cationic procedures [7–9]. Results of studies on the free radical copolymerization of vegetable oils and styrene indicated that this type of reaction is not viable for the preparation of materials because the carbon-carbon unsaturations in vegetable oils are not sufficiently reactive [10]. However, highly unsaturated and conjugated vegetable oils and reactive comonomers in the presence of a cationic initiator, such as boron trifluoride/diethyl etherate, produce thermosets polymers with good mechanical and/or functional properties, depending on the initial reactive mixture and the polymerization conditions [11].

Among oils that can be used in cationic copolymerization, tung oil is particularly attractive due to its highly unsaturated structure (large number of reactive functionalities) with three conjugated carbon-carbon double bonds (greater reactivity toward cationic copolymerization) [12,13].

Aging of natural oil-based thermosets has usually been studied using different analytical techniques such as infrared spectroscopy, mechanical and thermo-mechanical analysis [14–19]. On the other hand, there is scarce information on the aging process of this kind of polymers focused on the structural changes at molecular level.

Since the '70s, positron annihilation lifetime spectroscopy (PALS) has been recognized as the unique technique that makes it possible a direct measurement of the sub-nanometer sized free volumes (v_h) in polymers, with the additional advantage of being a non-destructive technique [20]. In the literature, there are several works in which PALS has been used to study bio-based polymers (see for example [21–23]); but, only few works are addressed to the study of polymers derived from vegetable oils [24,25]. In particular, we recently reported PALS results obtained from the study of the effect of the composition and chemical aging in tung-oil-styrene networks [15]. In that work, experimental data obtained by means of dynamic-mechanical analysis were also reported. For all the samples prepared using cationic polymerization of tung oil and different concentrations of styrene, we observed that in the samples aged for two years at RT the average nanohole free volume decreased and the glass transition temperature increased as compared with the fresh samples. Our results allowed us to attribute this behavior to the chemical changes linked to oxidative polymerization and degradative processes in the network structure.

In this work, the effect of the presence of different comonomers (synthetic and bio-based ones) or a modifier on the structural and thermal properties of tung oil-based thermosets was studied. A detailed study on the influence of the aging process on the nanostructure of the different networks prepared is also presented. The experimental results reported were obtained using Fourier transformed infrared spectroscopy, dynamic-mechanical analysis, positron annihilation lifetime spectroscopy and thermogravimetric analysis.

2. Experimental

2.1. Materials

A commercial tung oil (TO) supplied by Cooperativa Agrícola Limitada de Picada Libertad, Argentina was employed. The major fatty acid in this oil is α-elaeostearic acid (84 wt%) that presents three conjugated C-C double bonds.

For the transesterification reaction, methanol (99.98% pure, Biopack, Argentina), sodium hydroxide (97% pure, Anedra, Argentina) and sulfuric acid (98.5% pure, Anedra, Argentina) were used. Acrylatedepoxidized soybean oil (AESO) was purchased by Sigma-Aldrich (CAS-No: 91722-14-4). The following materials were purchased from Cicarelli Laboratory, Argentina: Divinylbenzene 80% pure (DVB), styrene 99.5% pure (St) and tetrahydrofurane 99% pure, (THF).Boron trifluoride diethyl etherate ($BF_3.OEt_2$), a chemical compound with 46–51% BF_3, was obtained from Sigma-Aldrich and used as the initiator of the cationic reaction.

3. Methods and techniques

3.1. Methyl ester (ME) synthesis from tung oil (TO)

The complete details of ME synthesis as well as its characterization were reported in a previous publication and it is summarized in the Scheme 1 [2]. In brief, for the synthesis, 300 mL of TO was mixed with 90 mL of methanol and 1.8 g of sodium hydroxide in a glass reactor with mechanical stirring for 45 min at 50 °C. In a separating funnel, two phases were obtained (one rich in ME and the other in glycerol). The ME was purified by washing with a 0.015 N sulfuric acid solution, and subsequent washings with distilled water until achieving neutral pH. Finally, the ME was dried using a rotary evaporator under vacuum for 2 h at 50 °C [24].

3.2. Cationic copolymerization of tung oil in the presence of a modifier (AESO) and comonomers (St, DVB, ME)

A bio-based modifier, acrylated epoxidized soybean oil (AESO) and bio-based and synthetic comonomers: tung oil methyl ester (ME), styrene (St) and divinylbenzene (DVB) were used to prepare crosslinked samples with a fixed weight ratio of tung oil/comonomer (or modifier) = 70/30. The structures of the different reagents used are shown in the Scheme 2.

The selected quantity of AESO, ME, St or DVB was incorporated to the TO and the mixture was stirred. This step was followed by the

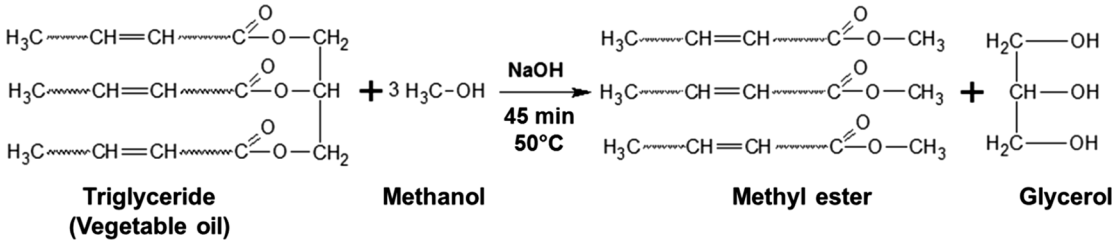

Scheme 1. Synthesis of methyl ester (ME) from a vegetable oil.

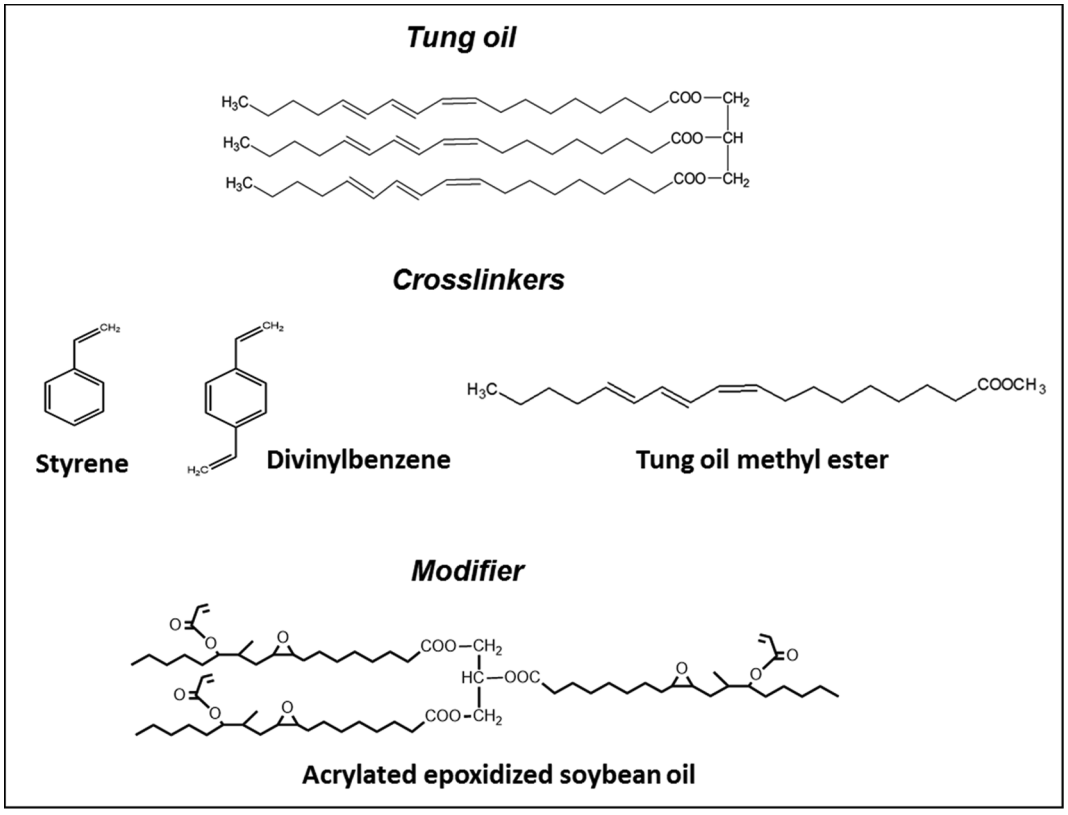

Scheme 2. Structure of the different reagents used in cationic copolymerization.

addition of the modified initiator prepared by mixing tetrahydofuran, THF (5 wt% with respect to the total reactive mass) with boron trifluoride diethyl etherate (3 wt% with respect to the reactive mixture) to obtain a homogeneous initial solution [10].The mixture was vigorously stirred and finally poured into glass plates of 13 × 18 mm^2 separated by a rubber cord of 1 mm of thickness and kept closed with metal clamps. The reactants were heated first at 25 °C for 12 h, then at 60 °C for 12 h and finally at 100 °C for 24 h. After reaction, part of the fresh samples (labeled as "F") were immediately tested and part of them were conditioned for 12 months in two different ways: at room temperature (RT) in a desiccator containing silica gel to maintain low humidity (samples labeled as "12M@RT") and in an oven at 50 °C (samples labeled as "12M@50C"). Schemes and additional discussions of the obtained networks were also included in previous publications [2,26,27].

Table 1 summarizes the composition of prepared materials and the nomenclature used to identify them after being subjected to different aging conditions. In the Scheme 3 a general graphical representation of the reaction between TO and crosslinker by cationic polymerization is shown.

3.3. Chemical characterization of the materials (FT-IR)

FT-IR spectra of the recently prepared samples ("fresh samples") were recorded by the attenuated total reflection method (ATR) using a Thermo Scientific Nicolet 6700 FT-IR spectrometer. The spectra were obtained over the range of 500–4000 cm^{-1} with a resolution of 2 cm^{-1} and averaged over 32 scans. A spectrometer FT-IR Spectrum 100 (Perkin Elmer) was used to record, by the attenuated total reflection method (ATR), the spectra of the "aged" samples. The spectra were obtained over the range of 500–4000 cm^{-1} with a resolution of 4 cm^{-1} and averaged over 16 scans.

3.4. Dynamical-mechanical tests (DMA)

An Anton Paar rheometer (model Physica MCR-301) equipped with a CTD 600 thermo chamber was used to determine the variation of the storage (G′) modulus and the damping factor (tan δ) with the temperature. Glass transition temperatures (T_g) were determined as the temperatures corresponding to the maxima of the damping peaks (tan δ). Torsion geometry was used with rectangular specimens of 20 × 5 × 0.5 mm^3. Measurements were performed as temperature sweeps in the range −60 °C to 200 °C at a heating rate of 5 °C/min. The frequency was kept at 1 Hz, and the applied deformation at 0.1%, which corresponds to the linear viscoelastic range for the samples.

Table 1
Composition of prepared materials and the nomenclature used.

Tung oil thermoset recently prepared	Tung oil thermoset aged 12 months at room temperature	Tung oil thermoset aged 12 months at 50 °C	Tung oil	Comonomer (or modifier)
TO/ME-F	**TO/ME-12 M@RT**	**TO/ME-12 M@50C**	70% wt.	30% wt. methyl ester
TO/AESO-F	**TO/AESO-12 M@RT**	**TO/AESO-12 M@50C**	70% wt.	30% wt. acrylated epoxidized soybean oil.
TO/St-F	**TO/St-12 M@RT**	**TO/St-12 M@50C**	70% wt.	30% wt. Styrene
TO/DVB-F	**TO/DVB-12 M@RT**	**TO/DVB-12 M@50C**	70% wt.	30% wt. divinylbenzene

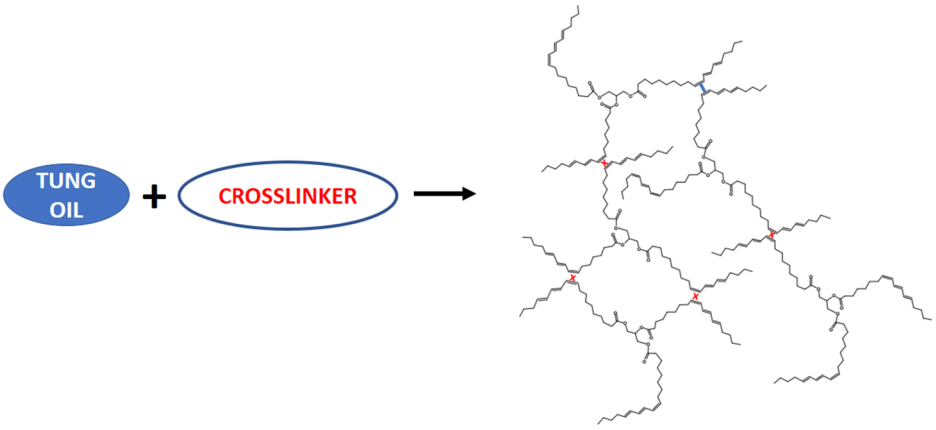

Scheme 3. Simplified graphical representation of the reaction between TO and crosslinker by cationic polymerization. Red crosses represent the links formed via the added crosslinker molecules, while the blue connector represents the direct reaction between oil double bonds. (For interpretation of the references to colour in this figure legend, the reader is referred to the web version of this article.)

3.5. Positron annihilation lifetime spectroscopy (PALS)

PALS measurements were carried out in air at RT using a fast-fast coincidence spectrometer with a lifetime resolution (FWHM) of 340 ps. A positron source (20 μCi) was prepared by the deposition of an aqueous ^{22}NaCl solution onto a thin Kapton foil (10 × 10 mm^2 and 7 μm thickness). After drying, the foil was covered with another piece of foil and the edges were glued with an epoxy resin. The source was sandwiched between two "identical" pieces of samples. PALS spectra containing around 1.5 × 10^6 counts were collected; at least ten spectra were taken for each sample and the obtained parameters were averaged.

All PALS spectra were resolved into three discrete lifetime components using the LT-10 analyzing program [28].

According to the common interpretation of PALS spectra in polymers, the nanoholes forming the free volume v_h can be directly estimated using a well-recognized semi-empirical equation through the long-lived lifetime component attributed to *ortho*-Positronium (o-Ps) annihilation by pick-off trapped into the holes; that is, $\tau_3 \cong \tau_{o\text{-}Ps}$. A correlation between the experimental input $\tau_{o\text{-}Ps}$ and the average size of the hole is possible assuming a spherical approximation of holes of radii R, as expressed using a simple quantum mechanical model; the Tao-Eldrup model [29,30]:

$$\tau_{o-\mathrm{Ps}} = 0.5\left[\frac{\Delta R}{R+\Delta R} + \frac{1}{2\pi}\sin\left(\frac{2\pi R}{R+\Delta R}\right)\right]^{-1}$$

where $\tau_{o\text{-}Ps}$ is given in ns and $\Delta R = 0.166$ nm is an empirical parameter valid for materials containing simple covalent bonds such as polymers [28]. The average nanohole free volume can then be calculated as:

$$v_h = \frac{4}{3}\pi R^3$$

3.6. Thermogravimetric analysis (TGA)

Thermogravimetric (TGA) studies were performed in a TGA-DTGA Q500 TA instrument from RT to 650 °C at 10 °C/min under air atmosphere to study changes due to the degradation process.

4. Results and discussion

Although the aging processes of bio-based networks have usually been studied using conventional techniques, they do not provide specific information on the nanostructure of these systems. Therefore, for the present work we made use of PALS that is considered to be the most sensitive experimental technique to follow the structural evolution of different materials at the nanoscale induced by thermal or thermo-mechanical treatments [31–33].

In this context, PALS was used for the first time to carry out a systematic study on the evolution of the free volume of nanohole in the different natural oil-based thermosets as a function of aging time. As a consequence, in a first step PALS results obtained for samples aged at RT indicated that still after one year the matrix structure at molecular level of the samples did not reach a steady-state (detailed information is given and discussed below in the section entitled Positron Annihilation Lifetime Spectroscopy). Consequently, PALS measurements were also performed on the same samples aged at a temperature above RT; that is, 50 °C. This temperature was chosen to accelerate the reactions responsible for the aging of the samples but low enough to avoid undesirable chemical reactions. Furthermore, at this temperature the nanostructural evolution during artificial aging is slow enough to get reliable PALS data in reasonable experimental times.

In this Section, the results are presented under the following sequence: first the chemical characterization of the samples is given; then dynamical-mechanical analysis results are presented; and finally, through the direct measurement of the nanohole free volumes, the nanostructural evolution of the polymer matrix is discussed.

4.1. FT-IR characterization

In Fig. 1(a)–(d), the FTIR spectra of the samples TO/ME, TO/St, TO/AESO and TO/DVB, recently prepared and aged under different conditions are presented.

In the case of the "fresh" samples (results on the TO/ME and TO/St samples were already reported in Ref. [14]), the four spectra shown present a broad absorption band between 3000 and 3500 cm^{-1} assigned to the OH stretch vibration and which results from the partial oxidation of TO fragments in the networks occurred during curing [26]. In the region of 2850–3000 cm^{-1} appear the peaks that correspond to the CH stretch of the alkydic chains of the TO. Besides, the double peak located into the region between 1700 and 1750 cm^{-1} corresponding to the carbonyl absorption can be assigned to the presence of acid and ester groups in the tung oil.

In particular, the spectra of the "fresh" samples prepared with the synthetic comonomers (St and DVB) show the characteristic absorption peaks corresponding to the aromatic ring. The small peaks that appear close and above 3000 cm^{-1} correspond to aromatic CH stretch absorption, while the peaks at ~1500 and ~1620 cm^{-1} correspond to the aromatic C=C stretch absorption. Finally, in the spectra obtained for the sample TO/St, the peaks located at 675–750 cm^{-1} are assigned to the absorption of the aromatic out-of-plane (oop) bending vibration of the mono-substituted benzene ring. The bands appearing in the spectrum obtained for the TO/DVB "fresh" sample also correspond to the oop vibration of DVB and in that particular case, they suggest that the comonomer is mainly a *meta*-DVB.

As can be observed in Fig. 1(a)–(d), the effects of aging on all the samples are qualitatively similar for aging at RT or 50 °C, although the changes in the absorbance are more important in the last case. In general, the aging process leads to the reduction of the band corresponding to the −OH absorption located in the 3000–3500 cm^{-1} region, as well as a

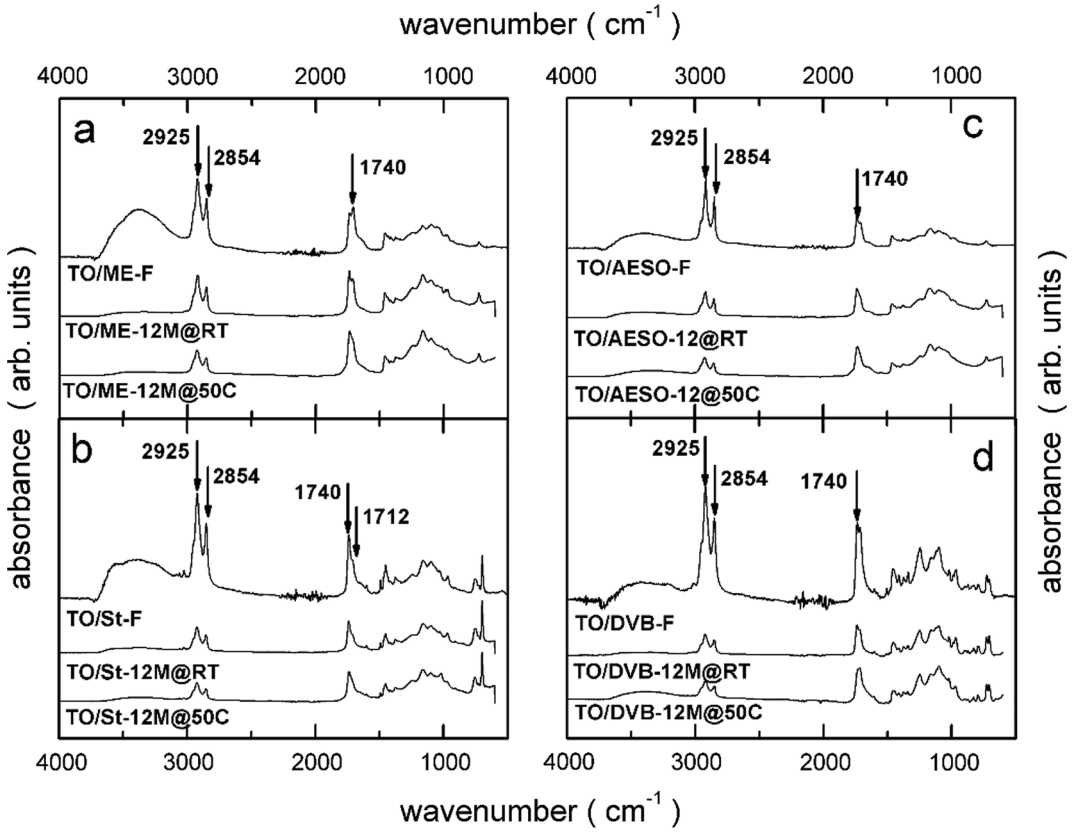

Fig. 1. Comparison FTIR curves corresponding to recently prepared and aged (for 12 months at RT in air atmosphere and 50 °C) samples.

decrease of the peak intensity (or shoulder depending on the sample) located at ~1710 cm^{-1}, which is assigned to carbonyl absorption and the 2900–3000 cm^{-1} bands. At this point, and in order to understand the reduction of the absorbance of the mentioned bands, a bibliographic revision addressed to this particular effect is given as follows.

The oxidation of unsaturated oils has been studied for years because of the negative tendency of edible oils to become rancid when exposed to oxygen and/or to heat for long time. As the material is exposed to the oxygen in the air, polar groups are formed, such as ether, carbonyl and hydroxyl groups. However, the overall change observed in the material is the result of the competing mechanisms of crosslinking and scission, both of them based on the initial incorporation of oxygen into the chemical structure of the material. Due to the scission processes, volatile materials like aldehydes, ketones, alcohols, short hydrocarbon chains, carbon dioxide and low molecular weight acids can be eliminated to the surroundings [34–36]. These small volatile molecules are formed from the scission of the unsaturated fatty acid moieties that remained unreacted or loosely attached to the network after the crosslinking reaction. However, and due to the competing rearrangement and crosslinking process, an increasing densification of these materials has been reported. All these reactions are known to proceed also in already formed films [33]. Studies of oil-based paint films have shown to contain products from the de-esterification of the triglycerides and/or degradation of the oxidized fatty acids. As the age of the films increased, a reduced concentration of these low molecular weight components has been measured [37].

Mallégol et al. [3] reported that during the autoxidation process of linseed oil cured at 60 °C, hydroperoxides were formed (related to the FT-IR absorption band centered at 3425 cm^{-1}) followed by the formation of alcohols, aldehydes, ketones, carboxylic acids and peresters. They also reported that the radical species, which were formed through different competing reactions, recombined to form crosslinked structures that were responsible for the cure of this particular drying oil. Juita *et al.* have also reported the liberation of volatile aldehydes, ketones, alcohols, carboxylic acids in the vapor space of oxidizing linseed oil [38]. Additionally, Irshad et al. [4] concluded that after an initial autooxidation step leading to peroxide generation, a drying oil goes through extensive crosslinking, which is further followed by a slow consumption of labile crosslinks to give rise to a more stable network structure.

Other authors have studied the changes that took place during UV irradiation under air atmosphere of a vegetable oil-based polyurethane [39]. Their observations also indicated that a mechanism consisting in the formation of hydroperoxides starts the process. The process continues with chain scission that also leads to the reduction of the intensity of the $-CH_2$ stretching vibration peak at about 2900 cm^{-1}, as well as the reduction of the intensity at ~1710 cm^{-1} due to the loss of alkyl groups in volatile carboxylic acids, aldehydes, etc. Changes in the intensity of peaks located in the 1000–1600 cm^{-1} (mainly those corresponding to C-O and C-H vibrations) were also observed, which are related to the loss of volatile components generated by scission of the chemical structures [39].

Besides the changes that vegetable oils can suffer during exposure to air, it must be taken into account that some of the samples (those cured with synthetic crosslinkers) contain aromatic moieties. Thus, the oxodegradation and crosslinking in the hybrid network TO/St was also considered. It is assumed that although the oil chains can react between themselves, most of the bonds occur through relatively short chains of St homopolymer. As far as we know, few publications discuss the degradation of polystyrene (PS) in the presence of vegetable oils, however, one article by Dong *et al.* reports on the degradation of PS in bean oil [40]. In that work, the authors found that the volatile products eliminated corresponded to products of the degradation of the bean oil, while fragments of PS were generated and remained in the solid phase [40]. According to those results, the higher the content of vegetable oil, the higher is the effect of the oxidation on the material, in consequence they observed that the oil segments were the ones responsible for degradation in air (not the St segments). Actually, the changes occurring in the 1700–1750 cm^{-1} region, which is a region of absorption for the oil fragments in the sample, support this statement, since the larger changes occur in the spectra of the TO/ME (see Fig. 1).

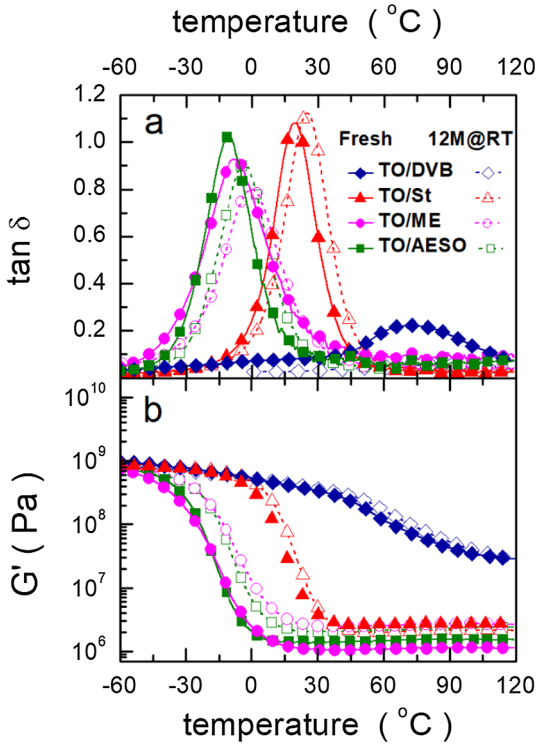

Fig. 2. Loss tangent tan δ (panel a) and shear storage modulus (panel b) curves as function of temperature obtained by DMA for copolymers fresh and aged for 12 months at RT.

On the basis of the results reported in the papers previously commented, it is clear that, due to the high content of TO in the molecular structure of the networks, the samples studied in the present work suffered similar processes to those described above. Thus, all the spectra of the aged samples show the reduction of the bands related to oxygen containing groups (3000–3500 cm^{-1} and ~1710 cm^{-1}) and also of the bands related to the lost alkydic segments (~2900 cm^{-1}).

4.2. Dynamical-mechanical analysis (DMA)

Dynamic mechanical properties tan δ and storage modulus are presented in Fig. 2(a) and (b), showing the effect of the monomer or modifier that was added to the reactive mixture of tung oil and a cationic initiator, as well as the effect of elapsed time on these properties (recently prepared and "aged" for 12 months at RT).

As discussed in a previous publication [2], the T_g values of the samples (arbitrarily taken as the temperature at the maximum in the tan δ curve) increase with time after the preparation independently of the modifier or the monomer added to the TO in the formulation. Thus, the change of T_g is associated with processes occurring on the TO segments that are present in all the samples studied.

After curing the reactive mixture of tung oil with DVB, St, AESO or ME in the presence of the cationic initiator, some carbon-carbon double bonds can remain unreacted in the structure. With time, the oxygen from the air diffuses into the samples and reacts with the polymer changing the crosslinking density as well as the number of dangling chains that act plasticizing the materials. Thus, the most important chemical reactions in the aging process are related to the oxidative polymerization and oxodegradation (chain scissions and formation of volatile products that are released to the ambient) [36]. In both cases, these reactions lead to the densification of the material, increasing its T_g.

The effect of the composition is clear in fresh or aged samples. The lowest T_g is observed for the sample of tung oil with AESO. As it is known and was mentioned in a previous publication [2], the AESO acts as modifier not as a crosslinker in cationic reactions. Consequently, as it could be expected, its effect is that of a plasticizer of the tung oil crosslinked network.

The addition of ME produces a slightly higher T_g in comparison with AESO (Fig. 2(a). ME is derived from TO through the transesterification of the oil. During this reaction, the unsaturations in the fatty acid chains are preserved and, further on, they participate in the cationic polymerization of the vegetable oil. However, even when ME acts as a crosslinker, the low equivalents *per* gram and the presence of free dangling chains introduce in the material a plasticizing effect that affects considerably the glass transition temperature. These two opposite effects result in negligible differences in the T_g values observed for the materials prepared with AESO and ME.

On the other hand, although styrene has a functionality of two, the rigidity of its aromatic ring contributes to reduce the mobility of the structure shifting the glass-rubber transition toward a higher temperature.

Finally, the highest T_g corresponds to the material prepared with DVB, which is very effective as crosslinking agent with a functionality equal to four in these polymerization reactions. This fact associated with its rigid molecular structure reduces the mobility of the final network.

The height and width of the tan δ peak have been associated with the nature of the network and its level of heterogeneity. According to this, the low height and large width of the tan δ curve of the material prepared with AESO, can be related to the heterogeneity of the crosslinked structure, which results from the direct reaction between the TO chains. Although such reaction would be favored by the oil chains having several functional groups per molecule, it would be unfavored by the sterical hindrance introduced by the structures being formed. Thus, one would expect tight crosslinking points coexisting with a high concentration of dangling chains and unreacted double bonds.

Fig. 2(b) shows the effect of aging on the shear storage modulus (G′) of the different materials. For those prepared with AESO, ME and DVB, aging leads to the increase of G' through the whole temperature range. As it was discussed above, different mechanisms of oxidative processes take place simultaneously, and one important change can be associated with the dangling segments of the fatty acid chains that act as plasticizers in fresh samples and can become part of the network after oxidative chemical reactions [37]. This structural change makes it possible the enhancement of the mechanical performance of the materials.

Notice that the largest change occurs in the rubbery plateau of the sample prepared with ME, since in that case all the chains (TO and crosslinker) are derived from the same vegetable oil and, thus, the whole material can suffer the oxidative densification reported in oil paints and films. Moreover, our results indicate that TO/ME is much affected by the oxidation, in both steps: formation of volatile compounds and rearrangement leading to crosslinking. On the other hand, the TO/St copolymer appears to suffer from the formation and evaporation of volatiles, but with St homopolymer segments contributing less to the formation of new additional crosslinking points, which is the reason for the relatively low value of the rubbery storage modulus of this sample.

Fig. 3 summarizes the results obtained for the glass transition temperature of the samples including the values obtained for the samples aged at 50 °C (one measurement). The observed trend is the same for all the samples, the glass transition temperature increases with aging, and the effect is stronger if the aging took place at a temperature above RT. This observation agrees with the discussion of the chemical changes observed by FTIR.

4.3. Positron annihilation lifetime spectroscopy

In Fig. 4, the evolution of the size of the nanoholes in the samples prepared with ME, AESO, St and DVB as a function of the natural aging time is presented. As can be seen, the v_h values corresponding to the

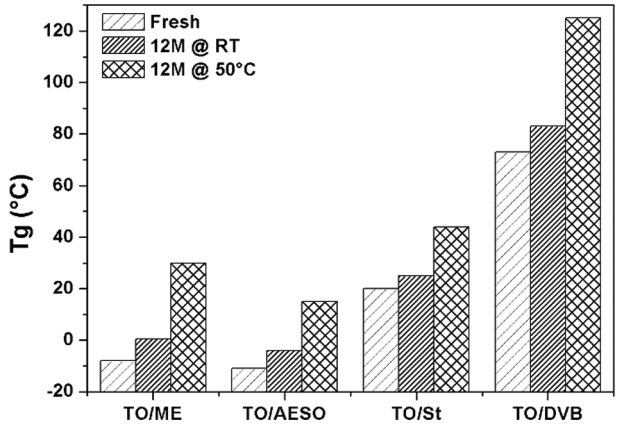

Fig. 3. T_g values from the fresh samples and aged for 12 months at RT and 12 months at 50 °C.

fresh samples (t = 0) are dependent on the comonomer or modifier used in the preparation of the samples. Specifically, the v_h values vary between ~120 Å^3 and ~155 Å^3 obtained for the TO/DVB and TO/ME samples, respectively.

From Fig. 4, it can be seen that the free nanohole volumes for the samples based only on components from natural sources (TO/ME and TO/AESO) coincide, within the experimental error.

On the other hand, for the samples containing petroleum-based comonomer: that is, St and DVB the v_h values are significantly lower than those obtained for the TO/ME and TO/AESO samples. These results suggest the formation of more closely packed structures, which are compatible with crosslinked samples prepared with the synthetic comonomers whose molecules are smaller than those of ME and AESO; or with the formation of short well-packed St homopolymer chains linking the TO as part of the structure of the networks.

Besides, the v_h obtained for the TO/DVB sample is lower than that of the TO/St network. Furthermore, as described above when discussing the DMA results, it is expected that the presence of two double bonds per molecule in DVB generates a more crosslinked network than that prepared with St.

In Fig. 4, it can be observed a systematic and slightly linear decrease of v_h obtained for all the samples with the increase of the aging time at RT. The trend of the evolutions of the different v_h *versus* natural aging time suggests that 12 months is not enough time to reach the final nanostructural condition of the samples. Consequently, and as mentioned above, PALS measurements were performed onto the same fresh

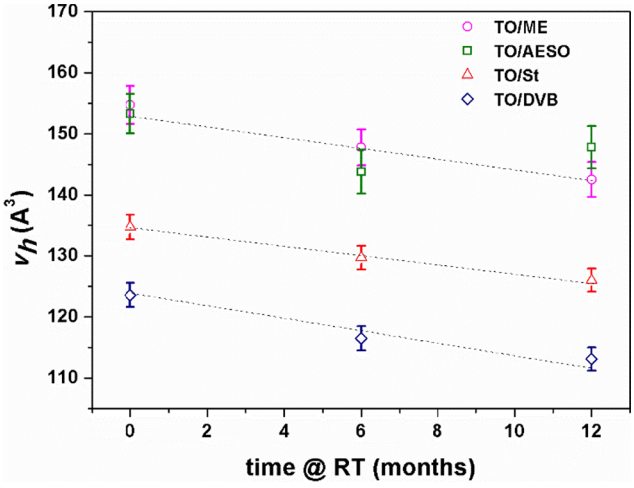

Fig. 4. Free nanohole volumes as a function of the aging time at RT for the different TO-based networks studied.

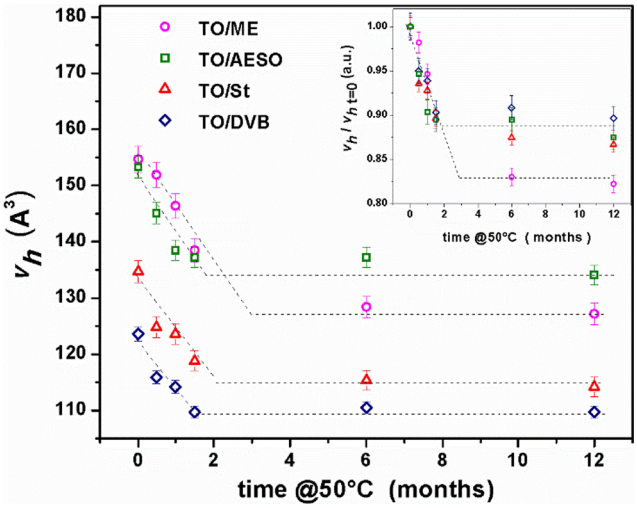

Fig. 5. Free nanohole volumes as a function of the aging time at 50 °C for the different TO-based networks studied. In the inset the data were plotted normalizing each data point to their own v_h value at t = 0 (see text).

samples but aged at 50 °C. In Fig. 5, the evolutions of v_h as a function of the accelerated aging time are presented. For all the studied samples, v_h values present a strong decrease for increasing aging times until approximately two months; then, for further aging times until one year the size of the nanoholes measured for each sample reaches, within the experimental scatter, a constant value.

It is important to point out that the v_h values at the *plateau*, obtained for each sample aged at 50 °C, are systematically lower than those measured in the samples aged for one year at RT. These results indicate that, using accelerated aging, it is possible to reach the equilibrium final nanostructural condition of the studied bio-based networks in about two months.

When the data points corresponding to each sample were normalized to its own v_h value of the "fresh" sample; that is, $v_h/v_{h\ t=0}$, it was found that for accelerated aging time between 0 and 2 months the normalized free volume data corresponding to all the samples can be well-fitted by a single linear function (see the inset in Fig. 5). From this result, it can be concluded that the mechanism involved in the structural changes at molecular level is the same for all the studied samples.

In the inset, it can also be seen that for artificial aging times longer than two months the $v_h/v_{h\ t=0}$ values corresponding to the TO/DVB, TO/St and TO/AESO samples can be well-fitted, within the experimental scatter, by the same straight constant function. This result indicates that the nanostructural steady-states reached for the three samples are equivalent. In the case of the TO/ME sample, the data points present a constant value approximately 10% below than the three samples previously mentioned. This difference can be attributed to the fact that comonomer ME is a molecule derived from the TO and, as such it undergoes the same oxidation mechanisms as the tung oil. Thus, all components in this particular sample suffer the oxidation effects. The relevance of the unsaturated oil fraction on the aging of this type of materials was previously reported [15] for TO/St samples with different TO/St ratios.

4.4. Thermogravimetric analysis (TGA)

Fig. 6 shows the thermogravimetric curves (TGA) of copolymers aged for 12 months at RT in air atmosphere.

A similar behavior with three degradation regions has been reported for other polymers obtained from natural oils [12,41,42], which in the present case appears in the temperature ranges of 150–300 °C, 300–520 °C and 520–800 °C. The first region is attributed to the evaporation of soluble, unreacted materials and the subsequent

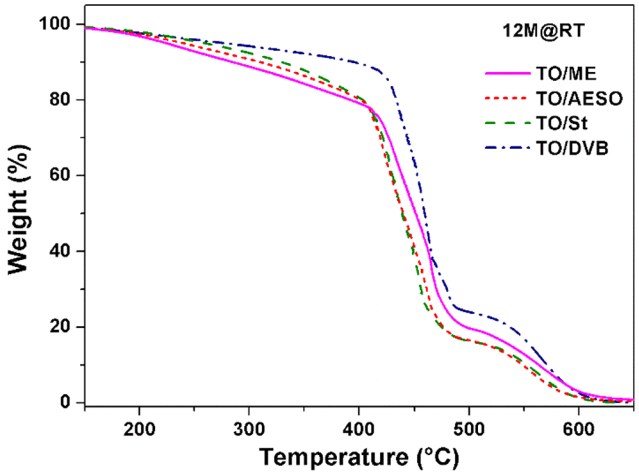

Fig. 6. Thermogravimetric curves (TGA) in air atmosphere of copolymers aged for 12 months at RT.

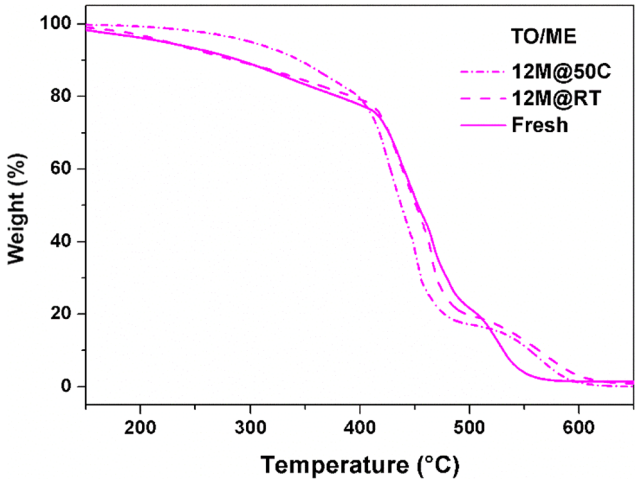

Fig. 7. Thermogravimetric curves corresponding to "fresh" and aged (12 months at RT and 12 months at 50 °C) TO/ME samples.

decomposition of free oil. These materials are the easiest ones to evaporate/degrade since they are not chemically bonded to the crosslinked network. The second region, related to the steepest slope, is due to the conversion of the structure of the crosslinked polymer to carbon. Finally, the third region above 520 °C, corresponds to the oxidation and degradation of the char as it evaporates/degrades in the air atmosphere. For all compositions, the carbonaceous residue is negligible at temperatures above 600 °C. The maximum rate of decomposition for all the samples is reached around 450–460 °C.

The results suggest that all the materials independently of the composition show qualitatively the same 3-stages degradation process, although differences are observed. In particular, in the degradation of the sample crosslinked with DVB, the second stage shows that the thermal degradation is delayed by the higher crosslinking density achieved in this network, since more covalent bonds must be broken for degradation to occur. Tighter DVB-network leads to the most thermally stable material and this can be observed in all three regions of degradation.

To further analyze the results of aging under the conditions considered (RT and T = 50 °C in air), in Fig. 7 comparative TGA curves obtained measuring the TO/ME samples are shown. Previous results made it possible to conclude that in comparison with the rest of the samples studied in the present work, the TO/ME copolymer presents the more significant changes when it is subjected to aging treatments.

Below 400 °C, thermal degradation shows that less material is lost from the aged samples, but this change is much more important in the sample stored at 50 °C, for which accelerated aging is expected. The lesser mass lost in this range of temperatures is explained by the occurrence of evaporation and decomposition of free oil and non-crosslinked fragments during storage. As explained in previous Sections, the samples suffered continuous loss of loosely bonded chains in the network structures, as well as the slow increase of crosslinking, both effects being the result of the oxidative aging of the oil fragments in the materials. This process is accelerated by aging at 50 °C and consequently, after one year the networks show a tighter crosslinked structure and lower loss of mass, particularly during the first degradation step.

Although the first and second steps of degradation are quite similar for the "fresh" sample and that aged at RT, the last step is shifted to higher temperature after aging. This is related to the fact that this copolymer presents a higher amount of TO derived components, which are the ones involved in the aging process.

5. Conclusions

The study of the changes produced in the networks prepared by cationic polymerization of tung oil, using different comonomers or adding a modifier, and aged at room temperature or at 50 °C (accelerated aging) makes it possible to conclude that the glass transition temperature as well as the free nanohole volume are strongly dependent on the nature of the comonomer (bio-based or synthetic) used to prepare the samples.

In addition, from the study of the nanostructural evolution of the samples subjected to accelerated aging two well-distinguished stages were observed. In the first one, from the fresh condition up to an aging time of two months *circa*, the rate of the chemical reactions is the same for all the samples, independently of the nature of the comonomers or modifier. For aging times longer than two months, the final nanostructural condition of the bio-based networks is reached. In particular, the nanostructural steady-states reached for the TO/DVB, TO/St and TO/AESO samples are equivalent. Additionally, the results obtained for the TO/ME sample, in which the comonomer ME is a molecule derived from the TO, allowed us to conclude that the oxidation mechanisms only occurs in the tung oil fraction of the bio-based polymer, independently of the used comonomer or modifier.

On the other hand, it was found that the oxidative process that affects unsaturated oils is also present in these samples (through any unreacted double bond), leading to the crosslinking of the carbon chains of the fatty acids and the progressive elimination of the produced volatile compounds of low molecular weight, which produce densification of the polymeric matrices.

CRediT authorship contribution statement

Sebastián Anbinder: Investigation, Visualization, Writing - original draft, Writing - review & editing. **Cintia Meiorin:** Investigation, Visualization, Writing - original draft, Writing - review & editing. **Carlos Macchi:** Investigation, Formal analysis, Writing - original draft, Writing - review & editing. **Mirna A. Mosiewicki:** Investigation, Conceptualization, Supervision, Funding acquisition, Writing - original draft, Writing - review & editing. **Mirta I. Aranguren:** Conceptualization, Supervision, Funding acquisition, Project administration, Writing - original draft, Writing - review & editing. **Alberto Somoza:** Conceptualization, Supervision, Funding acquisition, Project administration, Writing - original draft, Writing - review & editing.

Declaration of Competing Interest

The authors declare that they have no known competing financial interests or personal relationships that could have appeared to influence the work reported in this paper.

Acknowledgments

The authors thank the funding from the Agencia Nacional de Promoción Científica y Tecnológica (Argentina) (PICT 2016-2034, PICT 2015-1068 and PICT 2015-1832), Comisión de Investigaciones Científicas de la Provincia de Buenos Aires (Argentina), Secretaría de Ciencia, Arte y Tecnología – UNCPBA (Argentina) and Universidad Nacional de Mar del Plata (Argentina). The authors also thank the Cooperativa Agrícola de Picada Libertad (Argentina) for supplying the tung oil.

Data availability statement

Data not available / Data will be made available on request.

Appendix A. Supplementary material

Supplementary data to this article can be found online at https://doi.org/10.1016/j.eurpolymj.2019.109470.

References

[1] F. Li, R.C. Larock, Synthesis, structure and properties of new tung oil – styrene – divinylbenzene copolymers prepared by thermal polymerization, Biomacromolecules 4 (2003) 1018–1025, https://doi.org/10.1021/bm034049j.
[2] C. Meiorin, M.I. Aranguren, M.A. Mosiewicki, Polymeric networks based on tung oil: reaction and modification with green oil monomers, Eur. Polym. J. 67 (2015) 551–560.
[3] J. Mallégol, J.-L. Gardette, J. Lemaire, Long-term behavior of oil-based varnishes and paints I. Spectroscopic analysis of curing drying oils, J. Am. Oil Chem. Soc. 76 (1999) 967–976.
[4] A. Irshad, F. Delor-Jestin, P. Chalard, V. Verney, Physico-chemical durability criteria of oils and linked bio-based polymers, OCL 22 (2015) D107.
[5] A. Dupuis, F.X. Perrin, A. Ulloa Torres, J.P. Habas, L. Belec, J.F. Chailan, Photo-oxidative degradation behavior of linseed oil based epoxy resin, Polym. Degrad. Stab. 135 (2017) 73–84.
[6] D.A. Pratt, K.A. Tallman, N.A. Porter, Free radical oxidation of polyunsaturated lipids: New mechanistic insights and the development of peroxyl radical clocks, Acc. Chem. Res. 44 (2011) 458–467, https://doi.org/10.1021/ar200024c.
[7] G. Lligadas, J.C. Ronda, M. Galià, V. Cádiz, Renewable polymeric materials from vegetable oils: a perspective, Mater. Today. 16 (2013) 337–343, https://doi.org/10.1016/j.mattod.2013.08.016.
[8] C. Zhang, T.F. Garrison, S.A. Madbouly, M.R. Kessler, Recent advances in vegetable oil-based polymers and their composites, Prog. Polym. Sci. 71 (2017) 91–143, https://doi.org/10.1016/J.PROGPOLYMSCI.2016.12.009.
[9] F. Seniha Güner, Y. Yağcı, A. Tuncer Erciyes, Polymers from triglyceride oils, Prog. Polym. Sci. 31 (2006) 633–670, https://doi.org/10.1016/J.PROGPOLYMSCI.2006.07.001.
[10] A.M. Fernandez, A. Conde, Monomer reactivity ratios of tung oil and styrene in copolymerization, Polym. Appl. Renewable-Resource Mater. Springer, US, Boston, MA, 1983, pp. 289–302, , https://doi.org/10.1007/978-1-4613-3503-0_18.
[11] D.D. Andjelkovic, M. Valverde, P. Henna, F. Li, R.C. Larock, Novel thermosets prepared by cationic copolymerization of various vegetable oils – Synthesis and their structure-property relationships, Polymer (Guildf). 46 (2005) 9674–9685 http://www.scopus.com/inward/record.url?eid=2-s2.0-26844436871&partnerID=40&md5=19fa1d06360ab29ef47cd5b7943f479c.
[12] F. Li, R.C. Larock, Thermosetting polymers from cationic copolymerization of tung oil: synthesis and characterization, J. Appl. Polym. Sci. 78 (2000) 1044–1056.
[13] C. Liu, X. Yang, J. Cui, Y. Zhou, L. Hu, M. Zhang, H. Liu, Tung oil based monomer for thermosetting polymers: synthesis, characterization and copolymerization with styrene, BioResources. 7 (2012) 447–463.
[14] M.A. Mosiewicki, O. Rojas, M.R. Sibaja, J. Borrajo, M.I. Aranguren, Aging study of linseed oil resin/styrene thermosets and their composites with wood flour, Polym. Int. 56 (2007) 875–881.
[15] C. Macchi, C. Meiorin, M.A. Mosiewicki, M.I. Aranguren, A. Somoza, Effect of the composition and chemical aging in tung oil-styrene networks: Free volume and dynamic-mechanical properties, Eur. Polym. J. 87 (2017), https://doi.org/10.1016/j.eurpolymj.2016.12.016.
[16] C. Meiorin, M.A. Mosiewicki, M.I. Aranguren, Ageing of thermosets based on tung oil/styrene/divinylbenzene, Polym. Test. 32 (2013) 249–255, https://doi.org/10.1016/j.polymertesting.2012.10.009.
[17] P.L. Nayak, Natural Oil-Based Polymers: Opportunities and Challenges, J. Macromol. Sci. Part C Polym. Rev. 40 (2000) 1–21, https://doi.org/10.1081/MC-100100576.
[18] J. Shakina, A. Muthuvinothini, Synthesis and characterization of cotton seed oil based biodegradable thermosetting polymers, J. Acad. Ind. Res. 3 (2015) 520.
[19] S.G. Tan, W.S. Chow, Curing characteristics and thermal properties of epoxidized soybean oil based thermosetting resin, J. Am. Oil Chem. Soc. 88 (2011) 915–923, https://doi.org/10.1007/s11746-010-1748-x.
[20] Y.C. Jean, Positron annihilation spectroscopy for chemical analysis: A novel probe for microstructural analysis of polymers, Microchem. J. 42 (1990) 72–102, https://doi.org/10.1016/0026-265X(90)90027-3.
[21] J. del Río, A. Etxeberria, N. López-Rodríguez, E. Lizundia, J.R. Sarasua, A PALS contribution to the supramolecular structure of poly(l -lactide), Macromolecules 43 (2010) 4698–4707, https://doi.org/10.1021/ma902247y.
[22] M. Roussenova, M. Murith, A. Alam, J. Ubbink, Plasticization, antiplasticization, and molecular packing in amorphous carbohydrate-glycerol matrices, Biomacromolecules 11 (2010) 3237–3247, https://doi.org/10.1021/bm1005068.
[23] K. Sofińska, J. Barbasz, T. Witko, J. Dryzek, K. Haraźna, M. Witko, J. Kryściak-Czerwenka, M. Guzik, Structural, topographical, and mechanical characteristics of purified polyhydroxyoctanoate polymer, J. Appl. Polym. Sci. 136 (2019) 47192, https://doi.org/10.1002/app.47192.
[24] T. Kavetskyy, O. Smutok, O. Demkiv, S. Kasetaite, J. Ostrauskaite, H. Švajdlenková, O. Šauša, K. Zubrytska, N. Hoivanovych, M. Gonchar, Dependence of operational parameters of laccase-based biosensors on structure of photocross-linked polymers as holding matrixes, Eur. Polym. J. 115 (2019) 391–398, https://doi.org/10.1016/J.EURPOLYMJ.2019.03.056.
[25] B.V. Suresh Kumar, Siddaramaiah, M.B. Shayan, K.S. Manjula, C. Ranganathaiah, G.V. Narasimha Rao, B. Basavalingu, K. Byrappa, Effect of zeolite particulate filler on the properties of polyurethane composites, J. Polym. Res. 17 (2010) 135–142, https://doi.org/10.1007/s10965-009-9299-2.
[26] C. Meiorin, M.I. Aranguren, M.A. Mosiewicki, Vegetable oil/styrene thermoset copolymers with shape memory behavior and damping capacity, Polym. Int. 61 (2012) 735–742, https://doi.org/10.1002/pi.3231.
[27] C. Meiorin, M.I. Aranguren, M.A. Mosiewicki, Smart and structural thermosets from the cationic copolymerization of a vegetable oil, J. Appl. Polym. Sci. 124 (2012), https://doi.org/10.1002/app.35630.
[28] D. Giebel, J. Kansy, A new version of LT program for positron lifetime spectra analysis, Mater. Sci. Forum. 666 (2010) 138–141, https://doi.org/10.4028/www.scientific.net/MSF.666.138.
[29] S.J. Tao, Positronium annihilation in molecular substances, J. Chem. Phys. 56 (1972) 5499–5510, https://doi.org/10.1063/1.1677067.
[30] M. Eldrup, D. Lightbody, J.N. Sherwood, The temperature dependence of positron lifetimes in solid pivalic acid, Chem. Phys. 63 (1981) 51–58, https://doi.org/10.1016/0301-0104(81)80307-2.
[31] A. Dupasquier, G. Kögel, A. Somoza, Studies of light alloys by positron annihilation techniques, Acta Mater. 52 (2004) 4707–4726, https://doi.org/10.1016/J.ACTAMAT.2004.07.004.
[32] M.A. Monge, A.J.A. Díaz, R. Pareja, Strain-Induced Changes of Free Volume Measured by Positron Lifetime Spectroscopy in Ultrahigh Molecular Weight Polyethylene, Macromolecules (2004), https://doi.org/10.1021/MA049103I.
[33] A. Picasso, A. Somoza, A. Tolley, Nucleation, growth and coarsening of γ′-precipitates in a Ni–Cr–Al-based commercial superalloy during artificial aging, J. Alloys Compd. 479 (2009) 129–133, https://doi.org/10.1016/J.JALLCOM.2008.12.068.
[34] C. Su, Fatty acid composition of oils, their oxidative, flavor and heat stabilities and the resultant quality in foods, Iowa State University, Digital Repository (2003), https://doi.org/10.31274/rtd-180813-12583.
[35] R. Van Gorkum, E. Bouwman, The oxidative drying of alkyd paint catalysed by metal complexes, Coord. Chem. Rev. (2005) 1709–1728, https://doi.org/10.1016/j.ccr.2005.02.002.
[36] M. Ahmed, J. Pickova, T. Ahmad, M. Liaquat, A. Farid, M. Jahangir, Oxidation of lipids in foods, Sarhad J. Agric. 32 (2016) 230–238, https://doi.org/10.17582/journal.sja/2016.32.3.230.238.
[37] J.D.J. Van Den Berg, Analytical chemical studies on traditional linseed oil paints, 2002. https://doi.org/10.1002/app.
[38] B.Z. Juita, E.M. Dlugogorski, J.C. Kennedy, Mackie, identification and quantitation of volatile organic compounds from oxidation of linseed oil, Ind. Eng. Chem. Res. 51 (2012) 5645–5652.
[39] S. Das, P. Pandey, S. Mohanty, S.K. Nayak, Investigation into the Influence of UV aging on green polyurethane/nanosilica composite coatings based on transesterified castor oil and palm oil isocyanate, J. Inorg. Organomet. Polym. Mater. 27 (2017) 641–657.
[40] D. Dong, S. Tasaka, N. Inagaki, Thermal degradation of monodisperse polystyrene in bean oil, Polym. Degrad. Stab. 72 (2001) 345–351.
[41] F. Li, R.C. Larock, Synthesis, structure and properties of new tung oil - Styrene - Divinylbenzene copolymers prepared by thermal polymerization, Biomacromolecules 4 (2003) 1018–1025.
[42] H. Handoko, Bio-based thermosetting copolymers of eugenol and tung oil, Iowa State University, 2014.